# Tri-Level Linear Programming Model for Automatic Load Shedding Using Spectral Clustering

Mario D Baquedano-Aguilar, Arturo Bretas, Nader Aljohani, Sean Meyn

# Tri-Level Linear Programming Model for Automatic Load Shedding Using Spectral Clustering

Mario D. Baquedano-Aguilar*, Arturo Bretas†‡, Sean Meyn*, Nader Aljohani§
*Department of Electrical & Computer Engineering, University of Florida, Gainesville, FL, USA
†Distributed Systems Group, Pacific Northwest National Laboratory, Richland, WA, USA
‡G2Elab, Grenoble INP, CNRS, Université Grenoble Alpes, 38000 Grenoble, France
§Department of Electrical Engineering, College of Engineering, Taibah University, Medina, Saudi Arabia
m.baquedanoaguil@ufl.edu, arturo.bretas@pnnl.gov, meyn@ece.ufl.edu, nzjohani@taibahu.edu.sa

***Abstract*—Traditional load shedding schemes can be inadequate in grids with high renewable penetration, leading to unstable events and unnecessary grid islanding. Although for both manual and automatic operating modes load shedding areas have been predefined by grid operators, they have remained fixed, and may be sub-optimal due to dynamic operating conditions. In this work, a distributed tri-level linear programming model for automatic load shedding to avoid system islanding is presented. Preventing islanding is preferred because it reduces the need for additional load shedding besides the disconnection of transmission lines between islands. This is crucial as maintaining the local generation-demand balance is necessary to preserve frequency stability. Furthermore, uneven distribution of generation resources among islands can lead to increased load shedding, causing economic and reliability challenges. This issue is further compounded in modern power systems heavily dependent on non-dispatchable resources like wind and solar. The upper-level model uses complex power flow measurements to determine the system areas to shed load depending on actual operating conditions using a spectral clustering approach. The mid-level model estimates the area system state, while the lower-level model determines the locations and load values to be shed. The solution is practical and promising for real-world applications.**

***Index Terms*—Automatic load shedding, intentional control islanding, linear programming, phasor measurement units, spectral clustering, state estimation.**

## I. Introduction

WITH the increasing penetration levels of distributed energy resources (DERs) and the decommissioning of conventional generating units due to efforts in decarbonization policies and grid modernization, power system operations are becoming highly complex [1]. DERs are typically connected through inverters, which poses technological challenges to grid operation [2]. Fast and reliable protection systems are crucial for stabilizing power system dynamics and preventing blackouts. Phasor measurement units offer opportunities for advanced wide-area measurement protection and control (WAMPAC) systems, but traditional hierarchical communication architectures might not meet real-time requirements.

Load shedding is the last resort to maintain system reliability and avert blackouts caused either by power capacity shortages or stability issues [3]. Current load-shedding schemes comprehend manual and automatic approaches [4], [5]. In manual operating mode, operators notify utilities of anticipated stressful conditions, leading to planned load shedding. Automatic load shedding otherwise employs under-frequency relays at substations. Loads are shed in predefined stages based on peak net load estimates. Although the existing framework has ensured reliability, it may yield sub-optimal outcomes in power grids with high renewable penetration. Advanced load-shedding solutions with centralized architectures face challenges in real-life applications due to communication technology latency.

To address these issues, [6] presented a bi-level linear programming model for automatic load shedding utilizing a distributed architecture while leveraging data from phasor measurement units (PMU). Although this model shows promising results for real-world applications, two strong assumptions were made: when determining system areas for load shedding, they were previously user-defined and after kept static. Regularly, determining areas to shed load requires the grid operator's knowledge of the system and system disturbance identification. However, recent advancements in related fields like intentional control islanding [7], have used the system topology, the admittance matrix, or transmission line ratings to pinpoint these areas [8], [9]. Nevertheless, these parameters remain constant in any power system and ignore the dynamic operating conditions introduced by DERs. To overcome this challenge, in this work PMU power flow measurements are considered in an upper-level model to determine system areas best to shed loads. Spectral clustering is used towards model solution. This information is then sent to a mid-level model, which employs a distributed weighted least squares constrained approach to estimate the system state. Decision variables at the mid-level model are then integrated into the lower-level model, which uses system estimated state to determine the optimal location and the load to be shed in each area. The key contributions of this work are:

- A formal linear programming tri-level model for under-frequency load shedding using a distributed architecture;
- The determination of optimal areas to shed load according to the system's actual operating and disturbance conditions.

The remaining of the paper is organized as follows. Section II presents the tri-level model. A study case using the IEEE 14-bus test system is presented in Section III, while

979-8-3503-1360-4/24/$31.00 ©2024 IEEE

conclusions and future research topics are contained in Section IV.

## II. Tri-Level Model

The proposed tri-level linear programming model is composed of upper-level, mid-level, and a lower-level model. A schematic illustration is shown in Fig. 1. In contrast to traditional algorithm execution on a centralized computer that has communication capabilities with the load-shedding relays, we envision our application on an energy management system (EMS) that will be running in the server of the utility considering critical infrastructure protection (CIP) zones. The North American Electric Reliability Corporation (NERC) defines the CIP zones to ensure the protection of assets used to operate North America's bulk electric systems.

### A. Upper-Level Model

The upper-level model estimates best system areas to shed load according to operating and disturbance conditions. These areas are determined and continuously updated in less than $t < 90$ms complying with the range of PMU processing times [10]. To avoid communication issues during fault events, the model uses the most recent set of PMU power flow measurements prior to a disturbance to construct the network's graph representation, which is essential for area determination.

*1) Determining $k$-Shedding Areas:* To determine areas where load can be shed according to actual operating conditions, we first need to build the power flow-based graph Laplacian matrix $W$. For this, we represent the power grid as an undirected graph, denoted as $G = (\mathcal{V}, E)$. The set of buses is $\mathcal{V} = \{1, 2, ..., n\}$, where $n$ is the total number of buses. The set of edges is $E \subset \mathcal{V} \times \mathcal{V}$, where $(i, j) \in E$ represents an edge connecting buses $i$ and $j$. Edges can be transmission lines or transformers. For a network with $n$ buses, the weighted adjacency matrix of the graph is

$$W = \begin{pmatrix} 0 & \omega_{12} & \cdots & \omega_{1n} \\ \vdots & \vdots & \ddots & \vdots \\ \omega_{n1} & \omega_{n2} & \cdots & 0 \end{pmatrix}, \tag{1}$$

where $\omega_{ij}$ represents an edge weight as a non-negative function $\omega : \mathcal{V} \times \mathcal{V} \rightarrow \mathbb{R}^+$ such that

- $\omega_{i,j} = 0$ if $(i, j) \notin E$, i.e., vertices $i$ and $j$ are not connected by and edge.
- $\omega_{i,j} = \omega_{j,i}$ if $i \neq j$, i.e, edge directions are ignored since $G$ is undirected.

**Power Flow Weighted Matrix.** In this work, complex power flow (in MVA) measurements are used to define edge weights. To avoid any specific weight from leading to inaccurate clustering results due to fluctuating operating conditions reflected in the complex power flow magnitudes, we transform the resulting matrix $W$ into a normalized Laplacian matrix.

**Graph Laplacians.** In this work, we use the *normalized* symmetric graph Laplacian matrix $L_n$, which is commonly employed for clustering purposes (see [8], [9] and references therein). The entry-wise definition of both the *unnormalized* (2) and *normalized* (3) graph Laplacian matrices follows:

$$L_{ij} = \begin{cases} d_i & \text{if } i = j \\ -1 & \text{if } i \text{ is adjacent to } j \\ 0 & \text{otherwise,} \end{cases} \tag{2}$$

where $d_i = \omega(i, i) = \sum_{j=1}^{n} \omega(i, j)$ is the degree of the $i$th vertex. This is closely related to the adjacency matrix and is sometimes written as $L = D - W$, where $D$ is defined as the diagonal matrix with weighted vertex degrees $d_1, \cdots, d_n$ on the diagonal (i.e., $d_i$). The normalized graph Laplacian matrix $L_n$ is defined as:

$$L_n = D^{-1/2} L D^{-1/2} = I - D^{-1/2} \times W \times D^{-1/2}. \tag{3}$$

The eigenvalues of the normalized Laplacian matrix satisfy the inequality $0 \leq \lambda_i^{L_n} \leq 2$ for all $i$ [11]. The interested reader is referred to [9] for a detailed explanation of the preference of $L_n$ over $L$ in the power systems area.

*2) Choice of Dimension:* In situations where information such as the number of coherent groups of generators in the system is limited, a typical approach to determining the number of areas to shed load involves calculating the ratio of the absolute value of the difference between two consecutive eigenvalues of $L_n$ and their size. This parameter serves as a similarity measure known as the relative eigengaps [11]:

$$\gamma_{k,rel} = \frac{|\lambda_{k+1} - \lambda_k|}{\lambda_k} \quad (k \geq 2). \tag{4}$$

The presence of favorable $k$-areas is indicated by a small value of the $k$th eigenvalue, denoted as $\lambda_k$ in the graph Laplacian. Then, a high value of $\gamma_{k,rel}$ means that a minimum of $k$-shedding areas can be determined. This characteristic is expected to be evident through the spectral embedding in the $k$-dimensional space.

*3) The Algorithm:* In this work, we use the normalized spectral clustering algorithm according to [12] with some minor modifications.

**Algorithm 1** The Spectral Clustering Algorithm.

INPUT: Matrix $\mathbf{W} \in \mathbb{R}^{\mathbf{n} \times \mathbf{n}}$; parameter $k$.
**Compute the normalized Laplacian** $L_n$.
**Compute the eigenvectors** $v_1, \cdots, v_k$
of the generalized eigenproblem $L_n v = \lambda D v$
and take the first $k$ eigenvectors
**Let** $V \in \mathbb{R}^{n \times k}$ be the matrix containing the vectors $v_1, \cdots, v_k$ as columns.
**For** $i = 1, \cdots, n$ **let** $y_i \in \mathbb{R}^k$ be the vector corresponding to the $i$th row of $V$.
**Cluster the points** $(y_i)_{i=1,\cdots,n}$ in $\mathbb{R}^k$ with $k-$means or agglomerative clustering into areas $C_1, \cdots, C_k$.
OUTPUT: **Areas** $A_1, \cdots, A_k$ with $A_i = \{j | y_j \in C_i\}$

### B. Mid-Level Model

This model estimates the system state in each of the $k$ areas determined by the upper-level model. For a power system

979-8-3503-1360-4/24/$31.00 ©2024 IEEE

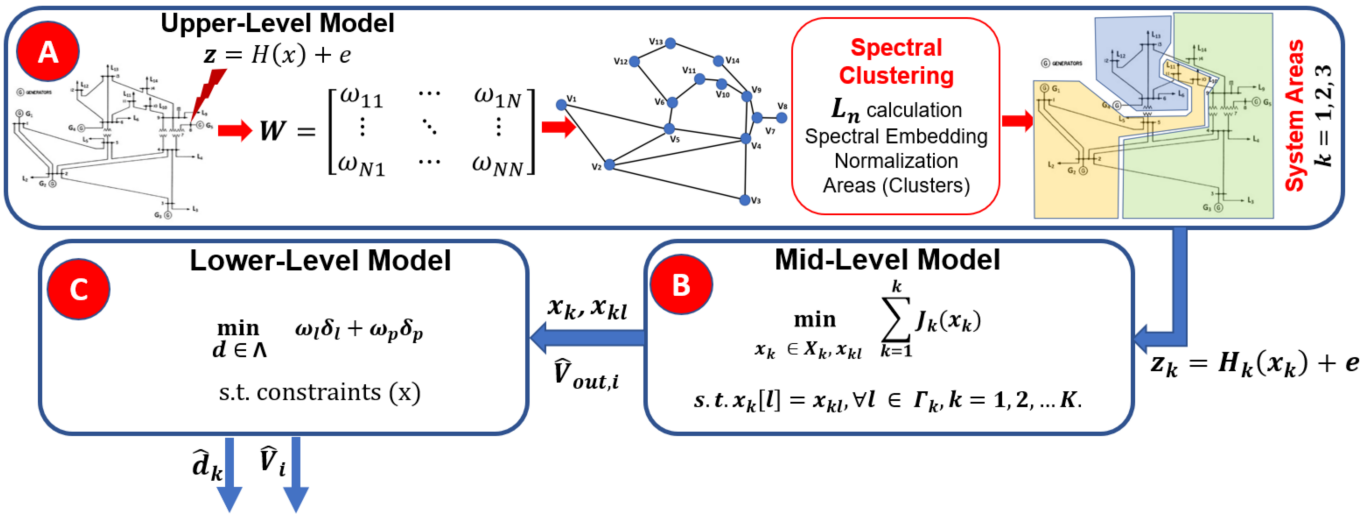


Fig. 1. The Tri-level model for automatic load shedding using linear programming and spectral clustering.

comprised of $n$ buses and $m$ measurements, it is possible to represent it as a collection of linear algebraic equations, as follows (see [6] and references therein):

$$z = H(x) + e, \tag{5}$$

where $z \in \mathbb{R}^m$ is the measurement vector, $x \in \mathbb{R}^N$ is the state variables vector, $H(x) : \mathbb{R}^N \longrightarrow \mathbb{R}^m, (m \geq N)$ is a linear function that relates the states to the measurements, and $e$ is the measurement residual vector with a Gaussian probability distribution, zero mean, standard deviation $\sigma$, and $N$ state variables such that $N = 2n - 1$. We can now write (5) for $k$ areas, $n$ buses, and $m$ measurements as follows:

$$z_k = H_k(x_k) + e. \tag{6}$$

The distributed weighted least squares (WLS) state estimator aims to find optimal estimates of the system states $x_k$ by minimizing the objective function $J_k(x_k)$:

$$J_k(x_k) = e(z_k, H_k)^T * R_k^{-1} * e(z_k, H_k), \tag{7}$$

where in area $k$, the residual vector $e(z_k, H_k)$ is represented as $(z_k - H_k(x_k))$, and $R_k$ stands for the measurement covariance matrix of the $k$th area. $J_k(x_k)$ is essentially an $L_2$-norm in the measurements vector space $\mathbb{R}^{m_k}$ of area $k$. Notice that $R_k$ for each area is a symmetric positive definite matrix with diagonal elements determined by the magnitudes of the corresponding measurements. The mid-level model's decision variables consist of the voltage angles of the buses within each area. The overall objective cost function for the distributed state estimation architecture is obtained by summing up the individual objectives of areas $k = 1, 2, 3$.

$$\min_{x_k \in \chi_k, x_{kl}} \sum_{k=1}^{K} e(z_k, H_k)^T * R_k^{-1} * e(z_k, H_k) \tag{8}$$

### C. Lower-Level Model

The lower-level model utilizes the mid-level estimated system states to determine both the location and the load to be shed. The primary objective is to reduce the effects of load shedding in the system. This is quantified by calculating the mismatch between the current system state obtained from the mid-level model, and the estimated state after implementing load shedding. To achieve this, the $L_1$-norm of the difference between the current and the estimated system states is used. The multi-objective optimization formulation of [6] has a secondary goal: to minimize the load flows through the tie-lines of the $k$ areas. However, as a consequence of the spectral clustering approach, this additional goal is unnecessary since the algorithm already ensures that the system is divided into $k$ areas with tie-lines carrying the minimum complex power flow, resulting in minimal energy disruption. The interested reader is referred to [8] and references therein for a detailed explanation of determining system areas considering minimum power flow disruption. The formulation of the lower-level model corresponds to a constrained linear optimization problem, expressed as follows:

$$\begin{aligned} &\min_{d \in \Lambda} \omega_l \delta_l + \omega_p \delta_p \\ &s.t. \sum_{i=1}^{N} \sum_{j=1}^{N} |\Delta V_{ij} - g_l| = \delta_l \\ &\Delta V_{ij} = |\hat{V}_i - \hat{V}_j| + |\hat{V}_{out,i} - \hat{V}_i| + |\hat{V}_{out,j} - \hat{V}_j| \\ &S_{rs} - S_{rs}^{lim} \leq \delta_p; \quad \delta_p \geq 0 \\ &\sum_{i=1}^{k_l} d_i \geq 0.9 \sum_{i=1}^{k_l} d_{mid,i}; \\ &S = XV, \end{aligned} \tag{9}$$

where $\delta_l \in \mathbb{R}$ is the distance to the primary goal ($\hat{V}_{out,i}$ is the mid-level model decision variable of bus $i$, and $\hat{V}_i$ is the estimated system state after load shedding, and $g_l$ is a previously defined goal), $\omega_l$ is its normalizing weight; $\delta_p$ is a user-defined parameter, which represents the complex power flow violation over the limit for each tie-line connecting the $k$ areas modeled as a soft constraint that penalizes the objective function using a high value of $\omega_p$ so that every area adjusts its tie-line complex power flows to remain within the limits;

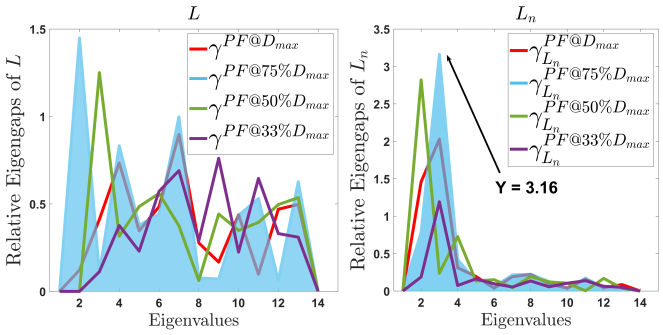


Fig. 2. The relative eigengap, $\gamma_{k,rel}$, of $L$ (left) and $L_n$ (right).

$\Lambda$ is the set of area loads; $S_{rs}$ is the complex power flow between buses $r$ and $s$; $S_{rs}^{lim}$ is the complex power flow limit between buses $r$ and $s$; $d \in \mathbb{R}^{k_l}$ is the load shedding vector, and $k_l$ is the area number of loads that can be shed; $d_{mid} \in \mathbb{R}^{k_l}$ is the load vector estimated from the mid-level model; $S \in \mathbb{R}^N$ is the intra-area complex power injection bus vector; $X : \mathbb{R}^{N-1} \rightarrow \mathbb{R}^m, (m > N)$, is a linear function that relates the states to the measurements; and $V \in \mathbb{R}^{N-1}$ is the state variables vector.

## III. Case Study

In this case study, the tri-level model is applied to the IEEE 14-bus system for three operating conditions: maximum, mid, and low demand. In all cases, the loss of the generator connected at bus 8 is considered. Each area is considered to have a measurement data set comprising 12 measurements obtained from GridSandbox [13]. This results in a local global redundancy level of four.

An under-frequency load shedding (UFLS) scheme is set to operate once the frequency drops below 59.5 Hz, 59.1 Hz, and 58.7 Hz by shedding 10% of the maximum demand with a time delay of 14 cycles between frequency thresholds. The preset value for $g_l$ in (9) is set to zero. All relay settings are adapted from PJM's automatic under-frequency relay setting program [14]. For the study case, islanding schemes are designed to activate after all three steps of the UFLS scheme have been executed, and the frequency drops to 58.5 Hz or below. This setting is based on the Southwest Power Pool's (SPP) automatic islanding scheme [15] for which no time-delay is considered as in [16].

**Obtaining the Number of Areas.** Complex power flow magnitudes in the system are used to update the weighted adjacency matrix $W$ described in Section II-A1. Then, the relative eigengaps of $L_n$ are computed as described in Section II-A2. Fig. 2 shows the relative eigengaps of $L$ (left) and $L_n$ (right) for the power flow-based Laplacian of the IEEE 14-bus test system for different operating conditions: maximum, mid, and low demand.

The maximum values of $\gamma_{k,rel}$ for the *unnormalized* and *normalized* Laplacians among all operating conditions are approximately 1.4 and 3.1 respectively. The violation of the inequality constraint in (4) indicates that the *unnormalized* Laplacian yields a poor similarity measure, aligning with findings in [8], [9], [17]. Therefore, we will also use the relative eigengaps of the normalized Laplacian matrix as a reliable similarity measure. Then, $\gamma_{k,rel}^{L_n} = 3.1$ suggests that -at least- $k = 3$ shedding areas can be determined.

**Determining the Buses by Area.** By knowing the number of areas we seek to find, the spectral clustering algorithm described in Section II-A3 can be implemented to determine and continuously update the system buses that belong to each area. The resulting areas to shed load for all operating conditions are depicted in Fig. 3 and specified in Table I.

TABLE I
Solution for $k = 3$ shedding areas based on three operating conditions: Maximum, Mid, and Low Demand.

| **Loading Level** | **Case A Demand = Max.** | | | **Case B Demand = 50%** | | | **Case C Demand = 33%** | | |
|---|---|---|---|---|---|---|---|---|---|
| **Areas: Blue/Green/Red** | **A1** | **A2** | **A3** | **B1** | **B2** | **B3** | **C1** | **C2** | **C3** |
| **Bus Number** | 6 | 7 | 1 | 4 | 6 | 1 | 6 | 1 | 3 |
| | 12 | 8 | 2 | 7 | 10 | 2 | 12 | 2 | 4 |
| | 13 | 9 | 3 | 8 | 11 | 3 | 13 | 5 | 7 |
| | 11 | 10 | 4 | 9 | 12 | 5 | - | 10 | 8 |
| | - | 14 | 5 | - | 13 | - | - | 11 | 9 |
| | - | - | - | - | 14 | - | - | - | 14 |

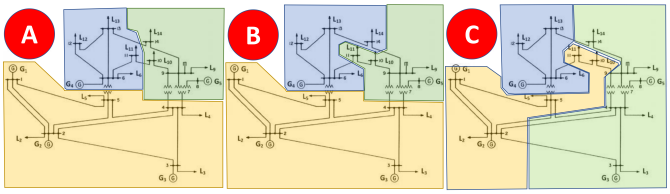


Fig. 3. $k = 3$ Shedding areas of the IEEE 14-bus system for three operating conditions via spectral clustering.

Due to the lack of space, the tri-level model for automatic load shedding is tested under a generator outage for the maximum demand operating condition only (see case A in Fig. 3 and Table I).

*1) Scenario A - Generator outage with traditional UFLS scheme:* After generator at bus 8 is lost (at $t = 1$ seconds), the frequency across the system rapidly drops, and complex power flows over branches 4-9, 5-6, and 13-14 increase, as shown in Fig. 4. Two of the flows exceed the threshold set for the relay,

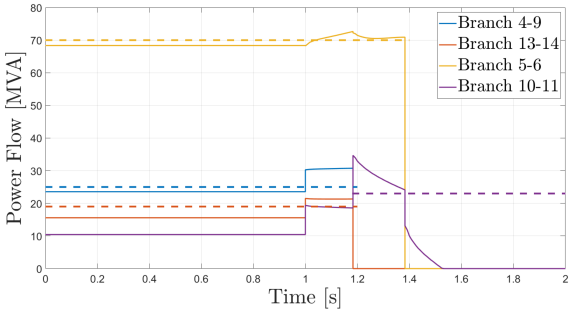


Fig. 4. Scenario A: The complex power flow magnitudes over tie lines.

which is indicated by dashed lines of the same color. After a short delay, these two tie-lines trip, causing another significant increase in the power flow magnitude of branch 5-6, causing it to trip as well. This leaves line 10-11 to be the only tie-line connecting the system, which is rapidly overloaded and trip. This cascading failure results in a frequency instability event

979-8-3503-1360-4/24/$31.00 ©2024 IEEE

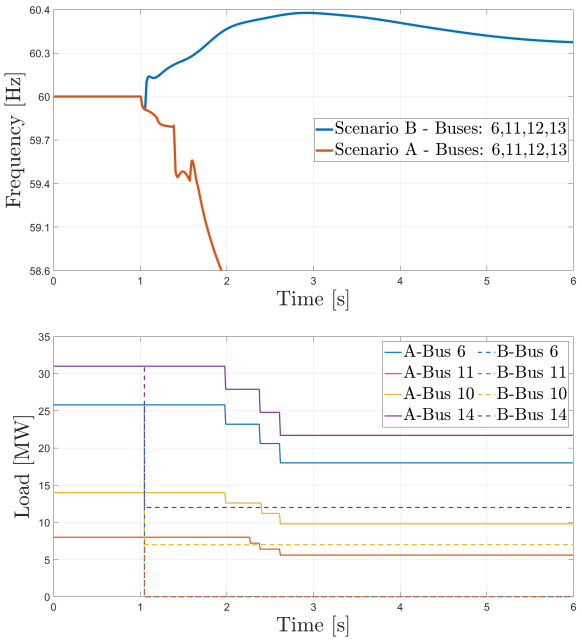


Fig. 5. Top: Frequency response for scenarios A and B. Bottom: Load shedding for scenario A (solid lines) and scenario B (dashed lines).

as shown in Fig. 5. This situation splits the system into three unstable islands, with frequency dropping as illustrated.

*2) Scenario B - Generator outage with the Tri-level automatic load shedding model:* With the same scenario as in $A$, the presented tri-level model would handle the event faster and more intelligently compared to a traditional UFLS scheme.

The tri-level model was able to proactively shed load at the most impacted buses to arrest system frequency prior to occurrence of significant deviations. As shown in Fig. 5, loads at buses 6 and 11 in Area 1, as well as the load at buses 10 and 14 in Area 2 (see Table I) are shed over several short steps. As we can see in Fig. 5 (see the frequency plot for scenario $B$), this scheme successfully prevents the cascading failure seen in the previous case, and brings the system frequency back to stable operation.

**Overshooting Drawback.** Given the fact that the tri-level model considers post-contingency predictive state estimates instead of frequency measurements, it continues to shed additional load so that islanding is still likely to occur due to line relaying, even though frequency appears to be recovering.

## IV. Conclusions and Future Work

In this work, a tri-level linear programming model for automatic load shedding to avoid system islanding using spectral clustering is presented. The upper-level model continuously updates the $k$ shedding areas considering minimum power flow disruption using a spectral clustering approach. The system state was estimated in the mid-level model by minimizing the sum of the $L_2$-norm of the measurement errors by area. The decision variables of this level were embedded into the lower-level model, which was formulated using a goal programming framework for which the primary goal was to minimize the impact of load shedding on the current system state. A traditional load shedding solution was built, which failed to respond quickly enough to prevent a cascading failure while the presented tri-level model was able to determine $k$ shedding areas depending on the current operating condition via a spectral clustering approach, identify the severity of the event, and shed load to avoid a system islanding situation.

**Topics for future research.** Areas of future work include adding a feedback control using the residual to correct the model to get a better estimate of the system states and solving the current overshooting issue as well.

## References


[1] J. Rockström, O. Gaffney, J. Rogelj, M. Meinshausen, N. Nakicenovic, and H. J. Schellnhuber, "A roadmap for rapid decarbonization," *Science*, vol. 355, no. 6331, pp. 1269–1271, 2017.

[2] A. Ulbig, T. S. Borsche, and G. Andersson, "Impact of low rotational inertia on power system stability and operation," *IFAC Proceedings Volumes*, vol. 47, no. 3, pp. 7290–7297, 2014.

[3] M. D. Baquedano-Aguilar, D. G. Colomé, E. Agüero, and M. Molina, "Impact of increased penetration of large-scale pv generation on short-term stability of power systems," in *2016 IEEE 36th Central American and Panama Convention (CONCAPAN XXXVI)*, 2016, pp. 1–6.

[4] Y. Omar, I. Abidin, S. Yusof, H. Hashim, and H. A. Rashid, "Under frequency load shedding (UFLS): Principles and implementation," in *2010 IEEE International Conference on Power and Energy*. IEEE, 2010, pp. 414–419.

[5] V. V. Terzija, "Adaptive underfrequency load shedding based on the magnitude of the disturbance estimation," *IEEE Transactions on power Systems*.

[6] A. Bretas, D. Wang, O. Vasios, and J. Ogle, "Bi-level linear programming model for automatic load shedding: A distributed wide-area measurement system-based solution," in *2023 IEEE Power & Energy Society Innovative Smart Grid Technologies Conference (ISGT)*. IEEE, 2023, pp. 1–5.

[7] J. Quirós-Tortós, R. Sánchez-García, J. Brodzki, J. Bialek, and V. Terzija, "Constrained spectral clustering-based methodology for intentional controlled islanding of large-scale power systems," *IET Generation, Transmission & Distribution*, vol. 9, no. 1, pp. 31–42, 2015.

[8] R. J. Sánchez-García, M. Fennelly, S. Norris, N. Wright, G. Niblo, J. Brodzki, and J. W. Bialek, "Hierarchical spectral clustering of power grids," *IEEE Transactions on Power Systems*, vol. 29, no. 5, pp. 2229–2237, 2014.

[9] M. D. Baquedano-Aguilar, S. P. Meyn, and A. Bretas, "Reduced-order models of static power grids based on spectral clustering," in *2023 North American Power Symposium (NAPS)*. IEEE, 2023.

[10] "IEEE Standard for Synchrophasor Measurements for Power Systems," *IEEE Std C37.118.1-2011 (Revision of IEEE Std C37.118-2005)*, pp. 1–61, 2011.

[11] F. R. Chung, *Spectral graph theory*. American Mathematical Soc., 1997, vol. 92.

[12] J. Shi and J. Malik, "Normalized cuts and image segmentation," *IEEE Transactions on pattern analysis and machine intelligence*, vol. 22, no. 8, pp. 888–905, 2000.

[13] H. M. Mustafa, D. Wang, K. S. Sajan, E. N. Pilli, R. Huang, A. K. Srivastava, J. Lian, and Z. Huang, "Cyber-power co-simulation for end-to-end synchrophasor network analysis and applications," in *2021 IEEE International Conference on Communications, Control, and Computing Technologies for Smart Grids (SmartGridComm)*, 2021, pp. 164–169.

[14] "PJM Manual 36," https://www.pjm.com/media/documents/manuals/m36.ashx, accessed: 2023-08-03.

[15] "SPP PC UFLS Plan," https://www.spp.org/documents/31556/spp%20pc%20ufls%20plan_rev_4.2_clean.pdf, accessed: 2023-08-03.

[16] M. D. Baquedano-Aguilar, N. Aljohani, S. P. Meyn, and A. Bretas, "Implementational aspects for the characterization of low-inertia in power systems," in *2022 North American Power Symposium (NAPS)*. IEEE, 2022, pp. 1–6.

[17] U. Von Luxburg, "A tutorial on spectral clustering," *Statistics and computing*, vol. 17, pp. 395–416, 2007.


979-8-3503-1360-4/24/$31.00 ©2024 IEEE